

Oyster patch reefs as indicators of fossil hydrocarbon seeps induced by synsedimentary faults

E. Hatem^a, N. Tribovillard^{a,*}, O. Averbuch^a, D. Vidier^b, P. Sansjofre^{c,1}, D. Birgel^d, F. Guillot^a

^a Université Lille 1, CNRS UMR Géosystèmes 8217, bâtiment SN5, 59655 Villeneuve d'Ascq cedex, France

^b PN82, rue du Calvairé, 62137 Coulogne, France

^c Equipe de géochimie des isotopes stables, Institut de Physique du Globe de Paris (IPGP), CNRS UMR 7154, Sorbonne Paris Cité, Univ Paris Diderot, 75005 Paris, France

^d Department for Geodynamics and Sedimentology, University of Vienna, Althanstrasse 14, A-1090 Vienna, Austria

ARTICLE INFO

Article history:

Received 11 June 2013

Received in revised form

12 November 2013

Accepted 9 December 2013

Available online xxx

Keywords:

Authigenic carbonates

Hydrocarbon seeps

Sulfate reduction

Late Jurassic

Boulonnais

Stable isotopes

ABSTRACT

The Late Jurassic deposits of the Boulonnais area (N-France) represent the proximal lateral-equivalent of the Kimmeridge Clay Formation; they accumulated on a clastic-dominated ramp subject to synsedimentary faulting as a result of the Atlantic Ocean rifting. In the Gris-Nez Cape area, i.e., close to the northern border fault zone of the Jurassic basin, the Late Jurassic sequence contains small-dimensioned oyster patch reefs (<1 m) that are specifically observed at the base of an abrupt deepening trend in the depositional sequence induced by well-defined pulses of normal fault activity. Petrographic analysis of these patch reefs shows that they are exclusively composed of *Nanogyra nana* embedded in a microsparitic calcite matrix. ^{13}C measurements, carried out within both the matrix and the shells, display significantly lower values in the matrix compared to the oyster shells which suggests that the carbonate matrix precipitation was involving a carbon source different from marine dissolved inorganic carbon, most probably related to sulfate reduction, which is evidenced by light ^{34}S in pyrites. Similarities but also differences with lucinid-rich bioconstructions, namely, the Late Jurassic pseudo-bioherms of Beauvoisin (SE-France) suggest that the patch reefs developed at hydrocarbon seeps are related to synsedimentary faults. The extensional block-faulting segmentation of the northern margin of the Boulonnais Basin in Late Jurassic times is thus believed to have induced a sort of small-dimension hydrocarbon seepage field, recorded by the patch reef distribution.

© 2013 Elsevier Ltd. All rights reserved.

1. Introduction

Fluid flow is a first-order feature of basin evolution. Expulsing fluids are interacting with sediments at the earliest stages of deposition, causing both early and late diagenesis of sediments. This is particularly crucial for basins subjected to extensional tectonic activity, where synsedimentary faults drive early diagenetic fluid circulations. These aspects are of cornerstone importance for petroleum systems. The geological formations of the Late Jurassic times (Kimmeridgian–Tithonian) crop out along the Boulonnais cliffs (Strait of Dover, Northern France; Fig. 1). They represent a proximal equivalent of the Kimmeridge Clay Formation (famous as

a major petroleum source rock) and they accumulated in a clastic-dominated ramp environment subject to dominantly aerobic conditions with some episodes of dissolved oxygen restriction favorable to organic-rich deposition (Wignall, 1991; Ramanampisoa et al., 1992; Proust et al., 1995; Al-Ramadan et al., 2005; Decoyninck et al., 1996; Wignall and Newton, 2001; Williams et al., 2001; Tribovillard et al., 2001, 2004, 2005). The Boulonnais is an excellent example of a small-dimensioned model of petroleum systems involving: 1) fine-grained, clay-dominated, organic-rich formations (termed “Argiles” in the local terminology, e.g., the Argiles de Châtillon Formation) acting as source rocks; and 2) coarser-grained, sandstone-dominated formations (termed “Grès”, e.g., the Grès de Châtillon Formation), acting as possible reservoir rocks. A recent study of the Bancs Jumeaux Formation suggested that synsedimentary tectonics induced fluid circulations through this incipient petroleum system, favoring carbonate precipitation and the formation of indurated carbonate beds, most likely stimulated by bacterial activity (Tribovillard et al., 2012).

* Corresponding author.

E-mail address: Nicolas.Tribovillard@univ-lille1.fr (N. Tribovillard).

¹ Present address: Université de Bretagne Occidentale, Laboratoire des Domaines Océniques, 29280 Plouzané, France.

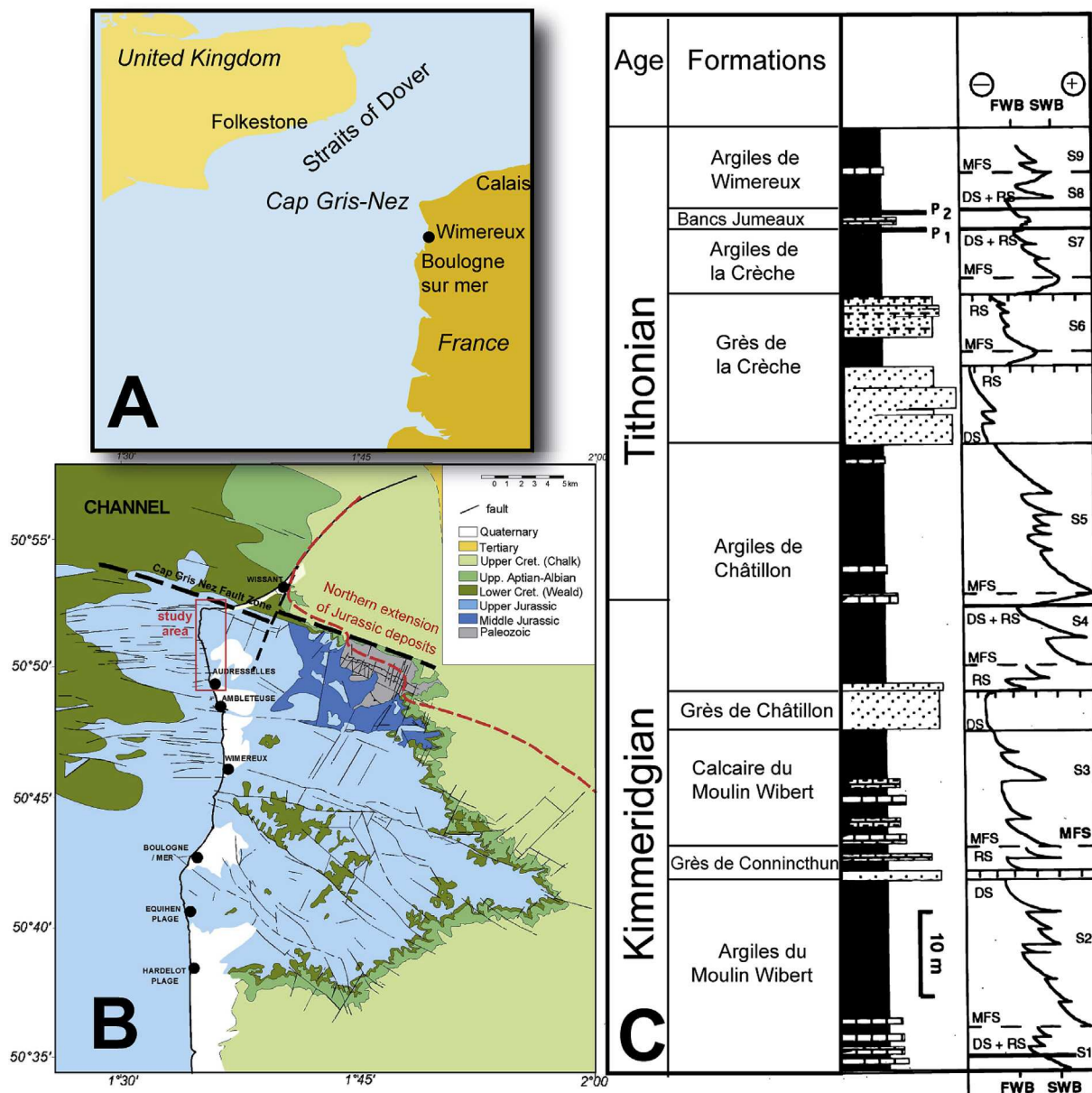


Figure 1. A – Large scale map showing the location of the study area, between the Gris-Nez Cape and the city of Wimereux. B – Geological map of the Boulonnais area (after Mansy et al., 2003). C – Simplified lithostratigraphic log of the Late Jurassic formations cropping alongshore the Boulonnais, showing the sequence stratigraphy framework (after Deconinck et al., 1996). FWB and SWB stand for fair-weather wave base and storm-weather wave base, respectively. P1 and P2 stand for the two horizons rich in phosphatized shells and pebbles.

From a structural point of view, the study area forms the eastern tip of the Weald-Boulonnais basin crossing through the English Channel along a general E–W direction. During the course of the entire Late Jurassic, this basin, alike the Wessex and the North sea basins, was affected by synsedimentary faulting in relation with the northward propagation of rifting along the Atlantic Ocean (Butler and Pullan, 1990; Underhill and Paterson, 1998; Beeley and Norton, 1998; Newell, 2000; Taylor and Sellwood, 2002; Hansen et al., 2002; Mansy et al., 2003; Minguely et al., 2010). This block-faulting geometry had a significant imprint on the subsidence pattern in the basin and, hence, on the depositional contexts. Along the Boulonnais cliffs, this resulted in significant lateral changes of sedimentary thickness and facies of the Kimmeridgian–Tithonian sequence indicating increasingly more proximal conditions toward

the North, up to the Gris-Nez Cape fault zone that represents the present northern onshore extension of the Jurassic deposits (Fig. 1B) (Mansy et al., 2003). One of the main expressions of these lateral depositional variations toward the Gris-Nez Cape fault zone is a progressive increase in the number and thickness of coquina beds into the dominant mudstone–sandstone sequence (Fig. 1C; a coquina is a detrital limestone composed wholly or chiefly of mechanically sorted shell fragments that experienced abrasion and transport before reaching the depositional site; cf., Bates and Jackson, 1987). Actually, in the Gris-Nez Cape area, the Late Jurassic formations contain numerous coquina beds, exclusively composed of the oyster *Nanogyra nana* and representing proximal tempestite deposits (Mansy et al., 2007). Recently, in addition to the coquina beds, occasional, ball- or dome-shaped assemblages of *N.*

nana were observed; they are small-dimensioned, *in situ* formed, oyster patch reefs (Fig. 2A–D and 3A–D; Mansy et al., 2007). The oysters *N. nana* are known to participate commonly to patch-reef building, notably during the Late Jurassic; however, in most patch reefs, *Nanoxyra* are accompanied by numerous other organisms, e.g., other genera of oysters, gastropods, serpulids, echinoids, bryozoa, foraminifera, sponges, etc. (e.g., Fürsich, 1981; Helm and Schulke, 1998; Delecat et al., 2001; Wilmsen et al., 2010). In contrast to the faunal composition of most Late Jurassic patch reefs, the Boulonnais patch reefs are rather small and isolated, and are only containing *N. nana* shells preserved in a carbonate-mud matrix (Figs. 2 and 3). The present study focusing on field observations, petrographic, geochemical and isotopic analyses aims at characterizing the development of these patch reefs within the general geological framework of the syn-rift Late Jurassic deposits. Integration of these data and their comparison with the well-studied Beauvoisin “pseudo-bioherms” (bioconstructions) that developed as well along synsedimentary faults in SE France (see section 6.2) will lead us to suggest that these specific ecosystems were controlled by localized fluid expulsion along fractures and faults, favoring bacterial activity at hydrocarbon seep sites through sulfate reduction.

2. The Late Jurassic oyster patch reefs of the Boulonnais: geological context

The Late Jurassic deposits of the Boulonnais form a ca. 100 m-thick sequence, mainly composed of alternating sandstones and black mudstone units as a primary result of the relative sea level oscillations (Fig. 1C). A brief description of the geological formations mentioned in the paper can be found in Table 1. A more detailed description of these formations, cropping out along the Boulonnais shore, may be found in Geyssant et al. (1993),

Deconinck et al. (1996), Proust et al. (1995), Mansy et al. (2007). The studied patch reefs are placed at numerous sites between Audresselles village and Gris-Nez Cape (i.e., in more proximal depositional setting) along two conspicuous stratigraphic horizons: on top of the Grès de Conninchun and Grès de Châtillon formations (see below). The largest patch reefs are cropping out along the beach of the Gris-Nez Cape (Mansy et al., 2007), where they may reach a size of 1 m (Fig. 2), whereas the usual size range of these objects is 10–50 cm.

1) The most common stratigraphic position by far for the patch reefs is the base of the Argiles de Châtillon Formation, a sequence predominated by organic carbon-rich mudstone, generally intercalated between two low-stand sandstone units, namely, the Grès de Châtillon Formation at the base, and the Grès de la Crèche formation at the top (Fig. 1C and Table 1). Both of these clastic-dominated formations mainly consist of brown-to orange-colored sandstones and sandy marlstones with common cross-bedding and wave ripples, as well as intense bioturbation (especially U-shaped and *Rhizocorallium* burrows). Along the cliffs north of Audresselles, some isolated 10–50 cm large patch reefs are observed *in situ* at the base of the first marlstone level of the Argiles de Châtillon, i.e., above an about 30 cm-thick siltstone bed, highly bioturbated, forming the top of the sandstone beds of the Grès de Châtillon Formation (Figs. 4 and 5). Overall, the patch reefs have been extracted from their caging marls by wave erosion and are found as cobbles or boulders directly on the top bed of the Grès de Châtillon on the beach, at the foot of the small cliff. In the Gris-Nez Cape site (“La Sirène” Beach), the Grès de Châtillon Formation does not exist under its common facies due to the more proximal depositional setting (the time-equivalent deposits are possibly lacking in the sedimentary record here). The base of the Argiles de Châtillon



Figure 2. A – Large, *in situ*, patch reef observed on the La Sirène Beach at the foot of the north cliff of the Gris-Nez Cape. B – A block, ripped off by wave erosion, from the large patch reefs of the La Sirène Beach. C – Close-up view of the patch-reef surface. D – A patch reef, smoothed by wave energy on top of a sandstone bed.

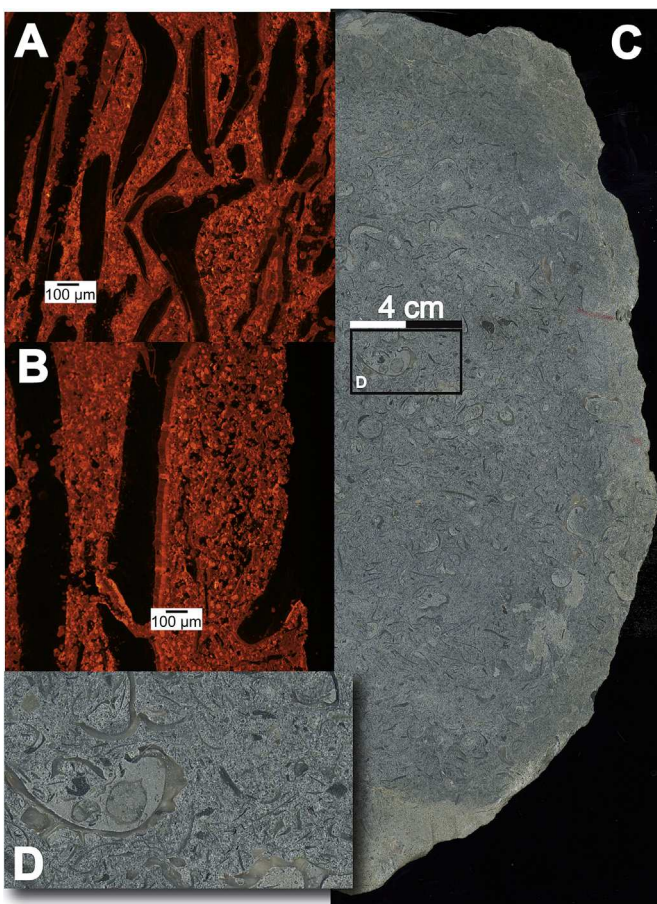


Figure 3. A & B – Cathodoluminescence imaging of thin sections showing the microspar of the calcite matrix and occasional fringes of larger crystals visible on some shells. The shells frequently show microborings. C – Large-scale view of a polished slab of a patch reef. D – Close up from C.

- Formation is marked by a spectacular 1–2 m thick ball-shaped oyster reef sequence (Fig. 2) that can be observed at numerous spots along the shore of the Gris-Nez Cape (Mansy et al., 2007). It is important to note that, at this site, the Late Jurassic rocks are intensely folded and dissected by faults due to their vicinity to the major fault zone of the Gris-Nez Cape (Fig. 1B) that controlled the subsidence pattern during the deposition of the Late Jurassic deposits (Mansy et al., 2003).
- 2) The second stratigraphic position of the observed patch reefs is much less extensive than the first one. This level is situated at the base of the Calcaires du Moulin Wibert Formation (Fig. 1C and Table 1), another mudstone dominated sequence containing, however, numerous carbonate beds. Two small-scale patch reefs were observed on the beach of the Gris-Nez Cape, directly on top of the sandstone bed forming the top of the Grès de Conninchun Formation (Fig. 6A–C).

3. Synsedimentary fluid circulations induced by tectonic activity?

Whatever the stratigraphic position of the observed patch reefs may be, it is noteworthy that they share common paleoenvironmental features. As exemplified by the general sequence-stratigraphy framework (Fig. 1C), the development of patch reefs corresponds to periods of rapid sea-level rise (i.e., at the base of the

Calcaires du Moulin Wibert Formation and at the base of the Argiles de Châtillon Formation). Furthermore, synsedimentary tectonic activity can be observed at the top beds of the sandstone units on which the patch reefs developed (i.e., the Grès de Châtillon and the Grès de Conninchun formations, respectively). Especially along the cliffs north of Audresselles (Fig. 4B), the Grès de Châtillon Formation shows very nice examples of meter-scale syndepositional, south-dipping, normal faults passing upward into a gentle flexure with recurrent southern subsiding panels filled up with sandstone or mudstone sequences of increasing thickness. This is also the case along the Gris-Nez Cape shore, where the top bed of the Grès de Conninchun Formation displays minor 10 cm-scale flexures in the vicinity of a more significant 10 m-scale north-dipping normal fault that also affects the overlying Calcaires du Moulin Wibert Formation (Fig. 6A).

Such observations strongly suggest that the sharp deepening trend at the base of the Calcaires du Moulin Wibert and Argiles de Châtillon formations is controlled by intense tectonic subsidence driven by recurrent pulses of normal fault activity. The related destabilization of the basin floor is likely to have promoted the expulsion of fluids from the deeper lying sediments, which could be a possible driving process for the development of the patch reefs at these specific stratigraphic intervals. The involvement of tectonic-induced fluids into the process controlling the development of observed patch reefs is strengthened by the observation of an isolated patch reef found directly on an N-dipping normal fault scarp just North of Audresselles (Fig. 5B–D). The Grès de Châtillon Formation that forms the footwall of this fault plane, yields very nice examples of sand injectites distributed normal to the fault plane, indicating the expulsion of fluids under pressure expelled away from the fault zone, as the sandstones were not cemented at the time of deposition (i.e., very early in the diagenetic course of the sand bodies).

To further constrain the nature and role of fluids possibly involved in the development of the patch reefs, we conducted a petrographical and geochemical study as explained below.

4. Methods

We characterized the patch reefs by means of petrographical and geochemical methods. Thin sections of the patch reefs were studied using a cathodoluminescence-equipped microscope (Olympus BX41 with a Citl 8200 MK4 cold-cathode cathodoluminescence device operating at 20 kV) and a scanning electron microscope (FEI Quanta 200 Environmental) equipped with a backscattered electron device and an energy dispersive spectroscopy-probe (X-Flash 3001 Brucker + Quantax 400 software). The carbonate content was determined with a Bernard-type calcimeter (acid digestion followed by CO₂ volume determination; accuracy < 5%). For stable carbon and oxygen isotope analysis, we sampled the shells, shell sparry fillings and the mudstone matrix using a micro-drill, to discriminate between the isotopic signatures of the various carbonate constituents of the patch reefs. The samples were further ground in an agate mortar and sieved to ensure grain size lower than 140 μm. CO₂ was extracted by calcite dissolution with 100% H₃PO₄ (McCreas, 1950) at 25 °C for 12 h in helium flushed Labco Exetainer® vials. Stable carbon and oxygen isotopic compositions of the evolved CO₂ were measured using a gas chromatograph coupled to an isotope ratio mass spectrometer (GC-IRMS) (Analytical Precision 2003, today entitled GV 2003, provided by GV Instruments), with helium as carrier gas. Three internal standards were used to calibrate the δ¹³C_{sample/ref} data provided by the GC-IRMS relative to the V-PDB scale and have been calibrated using two international standards, NBS19 and IAEA-CO1 (IAEA catalog). Results are given in the usual δ-notation relative to the

Table 1

Short description of the Late Jurassic geological formations of the Boulonnais.

Age	Ammonite zone	Formation	Short description
Encompassing the Kimmeridgian–Tithonian boundary	Autissiodorensis to Gigas-Elegans zones	Argiles de Châtillon	The formation consists of claystone and marlstone accumulations with two intervals of laminated paper shales and a laterally variable number of occasional intercalated limestone beds. The marlstones show a gradual enrichment in silt in the upper part of the formation. Storm beds are numerous, notably at the Kimmeridgian–Tithonian Autissiodorensis–Elegans zone) boundary.
Kimmeridgian	Eudoxus Zone, Contejeani subzone	Grès de Châtillon	The formation consists of brown- to orange-colored sandstones and sandy marlstones with common cross-bedding and wave ripples, and intense bioturbation (especially U-shaped and Rhizocorallium burrows).
Kimmeridgian	Eudoxus Zone, Contejeani subzone	Calcaires du Moulin Wibert	Irregular alternation of gray clay, more or less clear, and argillaceous limestones small beds (dm) and thicker beds (0.5–0.8 m). In the upper part of the unit, the beds are coquina.
Kimmeridgian	Eudoxus Zone, Caletanum–Contejani sub-zones	Grès de Connincthun	The formation is made up with a few sandstone beds that are rich in glauconite and large quartz grains. Abundant bivalves (<i>Trigonia</i>) and occasional echinoids are observed.

international standard V-PDB for $\delta^{13}\text{C}$ and $\delta^{18}\text{O}$. The external reproducibility for $\delta^{13}\text{C}$ and $\delta^{18}\text{O}$ measurements is of $+/-0.1\text{\textperthousand}$ and $+/-0.2\text{\textperthousand}$, respectively (1σ). Each sample was measured twice and the average of two analyses is reported in the figures.

To determine the stable sulfur isotope composition ($\delta^{34}\text{S}$) of pyrite, seven bulk rock samples of patch reefs were decarbonated through HCl digestion to concentrate pyrite. The decarbonated samples were oxidized with O_2 at $1050\text{ }^{\circ}\text{C}$ to produce SO_2 that was analyzed using a VG Sira mass spectrometer. The results were expressed in δ conventional notation, relative to the standard V-CDT (Vienna Canon Diablo Troilite). The standard was a Ag_2S

MERCK with $\delta^{34}\text{S} = +3\text{\textperthousand}$ vs. V-CDT. Each sample was measured in duplicate and the average values are reported. The analytical precision of measurements was $\pm 0.3\text{\textperthousand}$; the reproducibility was of $\pm 1\text{\textperthousand}$.

The mineralogical composition of the carbonate was determined using classical X-ray diffraction (XRD) of micro-pulverized samples (Bout-Roumazeilles et al., 1999). To that end, a Bruker D4 Endeavor apparatus was used together with the MacDiff software (Bout-Roumazeilles et al., 1999).

Three patch-reef carbonate specimens were chosen for lipid biomarker analysis and were prepared and decalcified after the method described previously (Birgel et al., 2006). After saponification with 6% KOH in methanol, the samples were extracted three times with a CEM Discovery microwave extraction system at $80\text{ }^{\circ}\text{C}$ and 250 W for 15 min with dichloromethane:methanol (3:1). For GC analyses, the total extracts were pre-cleaned by separation into an *n*-hexane soluble and dichloromethane-soluble fraction. The *n*-hexane fraction was further treated and separated by column chromatography into four fractions of increasing polarity (cf. Birgel et al., 2008). The hydrocarbon and carboxylic acid fractions were analyzed by gas chromatography-flame ionization detection (GC-FID) with an Agilent 7820 A GC system at the Department of Geodynamics and Sedimentology, University of Vienna. The GC-FID system was equipped with a 30 m HP-5 MS UI fused silica capillary column (0.25 mm i.d., 0.25 μm film thickness). The carrier gas was helium. The GC temperature program used for all fractions was: $60\text{ }^{\circ}\text{C}$ (1 min); from $60\text{ }^{\circ}\text{C}$ to $150\text{ }^{\circ}\text{C}$ to $320\text{ }^{\circ}\text{C}$ at $4\text{ }^{\circ}\text{C}/\text{min}$, 25 min isothermal. The aim was to verify whether characteristic microbial molecular fossils were preserved in the carbonates.

5. Results

5.1. Macrofacies

The patch reefs have a rounded shape and are composed of countless shells of *N. nana* that show no visible, preferential orientation. The two valves of the fossils are not always connected to each other. The shells are embedded in a limestone mud (Fig. 3A–D). No other fossils were identified, except for one individual gastropod. Overall, the patch reefs are indurated except for the largest ones, where some “seams” or fissures were observed. They are filled with abundant quartz grains and organic-rich matter. Most likely, these structures result from burrowing activity.

5.2. Microfacies

The various patch reefs at different stratigraphic levels showed the same microfacies features. The carbonate matrix is a

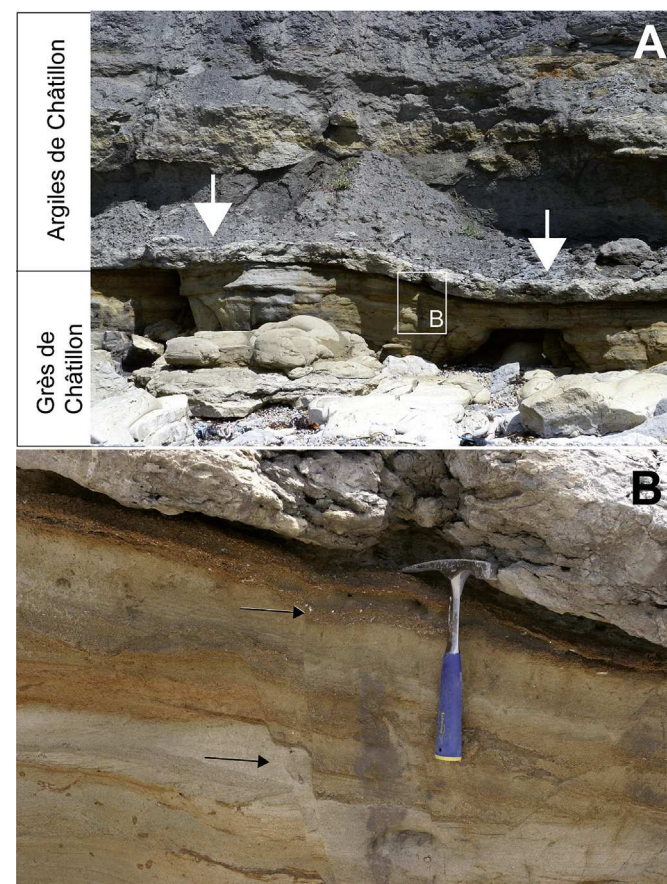


Figure 4. A – The white arrows point to the basal bed of the Argiles de Châtillon Formation, where the patch reefs are rooted. B – The black arrows show the synsedimentary faults visible in the upper part of the Grès de Châtillon Formation. Location: on the beach between the Gris-Nez Cape and the village of Audresselles: black cross in Figure 1B.

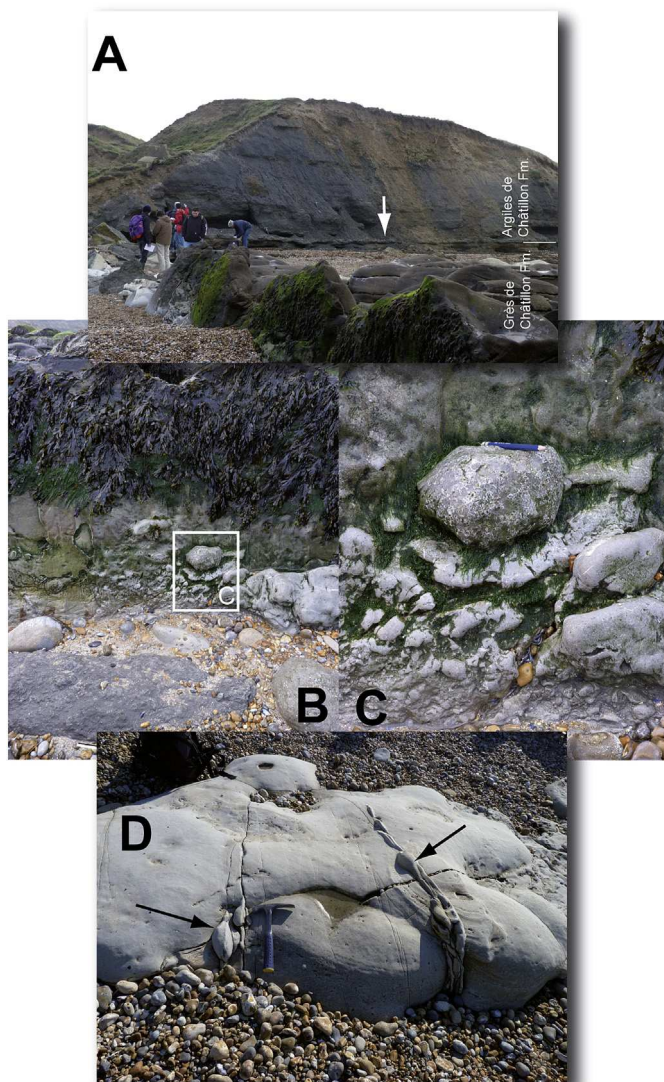


Figure 5. A – The white arrow indicates the basal bed of the Argiles de Châtillon Formation, as in [Figure 4A](#). The picture illustrates the Grès de Châtillon and Argiles de Châtillon formations. In the foreground, covered with green algae, the fault plane of a synsedimentary fault affecting the Grès de Châtillon Fm. On this plane, a small patch reef is rooted (B & C). The synsedimentary fault is accompanied by sand injectites visible in the Grès de Châtillon sandstone beds (D). Location: Cran du Noirda, the beach at the north end of Audresselles ([Fig. 1B](#)).

homogeneous calcite microspar with numerous shells and shell fragments, accompanied by common organic-rich particles and rare pyrite frambooids (packstone–grainstone fabrics; [Fig. 3A, B, D](#)). A fringe of sparitic crystals was frequently but not systematically observed around most shells ([Fig. 3A and B](#)). No coccolith fossils (or molds) could be observed. Cathodoluminescence imaging showed that in all observed thin sections, the color of the calcitic, microsparitic matrix is homogeneous. No luminescence contrast was observed, suggesting that the chemical composition of the carbonate matrix is homogeneous. Shells occasionally showed white, sparitic fillings. Regarding the mineralogy of carbonate, XRD data demonstrated that the microsparite of the matrix is composed of calcite.

5.3. Stable isotopes

The carbonate matrix samples (all but one) show $\delta^{13}\text{C}$ values ranging between -8.9‰ and -3.6‰ V-PDB, whereas both shell and

sparry shell-filling samples ranged between -2.0‰ and 0.6‰ V-PDB ([Fig. 7](#)). No distinction can be made between matrix samples, shell, and shell-filling samples when considering the $\delta^{18}\text{O}$ values ([Fig. 7A and B](#)). The range for all samples varies between -5.2‰ and -1.0‰ V-PDB. The two most-depleted samples correspond to shell

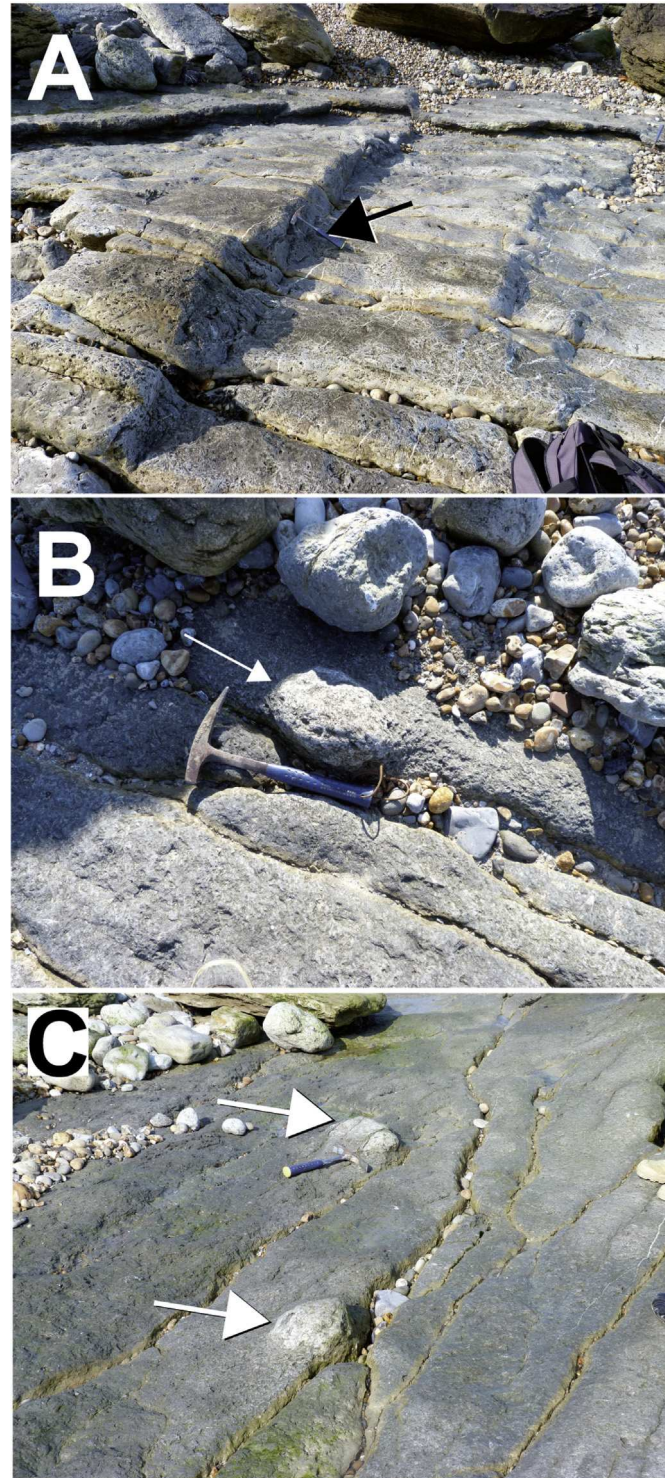


Figure 6. A – Synsedimentary, soft deformations affecting the top sandstone bed of the Grès de Conninchun Formation, producing sorts of stair steps. The black arrow shows the hammer. B & C: patch reefs rooted on the surface of this bed (white arrows). Location: La Sirène Beach, Gris-Nez Cape.

fillings. A positive correlation can be drawn, linking the CaCO_3 content to the $\delta^{18}\text{O}$ values (Fig. 7). For the seven samples ran for sulfur isotope composition of pyrite, the $\delta^{34}\text{S}$ values varied between $-42.9\text{\textperthousand}$ and $-35.1\text{\textperthousand}$ CDT (Fig. 7C).

At times, molecular fossils of prokaryotes (both bacteria and archaea) can be well preserved in Mesozoic authigenic carbonates (Peckmann et al., 1999; Birgel et al., 2006). Unfortunately, the overall lipid biomarker contents of the patch reef samples were very low and not diagnostic as being derived from bacteria and archaea in both the hydrocarbon and carboxylic acid fractions. Characteristic microbial biomarkers such as terminally-branched fatty acids (sulfate-reducing bacteria) or isoprenoid hydrocarbons

(methanogenic or methanotrophic archaea; see Peckmann and Thiel, 2004 for a review) were not identified or preserved. From the lipid biomarker results we were not able to make any conclusion on the contribution of microbes in the formation of the studied carbonates.

6. Discussion

6.1. Authigenesis in patch reefs

Within the patch reefs, the $\delta^{13}\text{C}$ isotope composition of the fine-grained carbonate matrix is varying significantly from the included

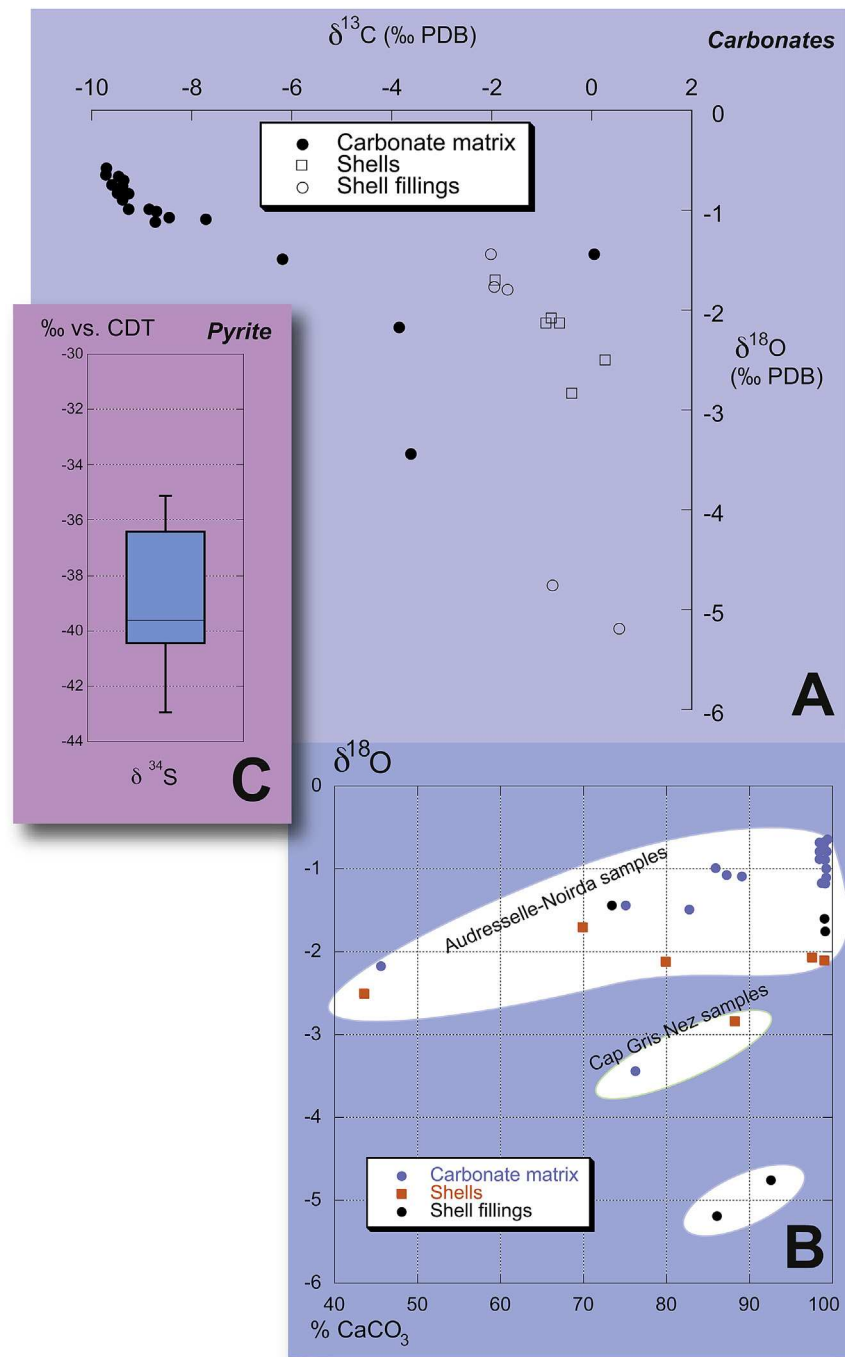
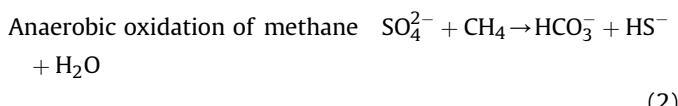
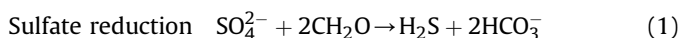
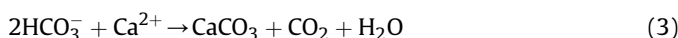


Figure 7. A & B – Carbon and oxygen stable isotope composition of the various carbonate fractions of the patch reefs. C – Box and whiskers-type diagram showing the S isotope composition of pyrite embedded in the patch reefs.

shells. The patch reefs are also varying isotopically from the enclosing marls. The basal marls of the Argiles de Châtillon Formation show $\delta^{13}\text{C}$ values ranging from $-0.2\text{\textperthousand}$ to $2.0\text{\textperthousand}$ (Tribovillard, unpublished data). Overall, the matrix samples are markedly depleted in ^{13}C , while the shell and sparry shell-filling samples resemble the values usually found in Late Jurassic seawater carbonates, which range from 0 to 2\textperthousand (Veizer et al., 1999; Prokoph et al., 2008). The $\delta^{13}\text{C}$ values of the carbonate matrix of the patch reefs are depleted in ^{13}C , pointing to another, more ^{13}C -depleted carbon source than dissolved inorganic carbon (DIC). It is inferred that the patch-reef matrix may be an authigenic carbonate incorporating a fraction of biogenic, ^{13}C -depleted carbon derived from microbial organic-matter remineralization during early diagenesis (cf. Berner, 1980; Folk and Chafetz, 2000; Peckmann and Thiel, 2004; Aloisi et al., 2002, and references therein). Microbes in sediments gain energy by performing various chemical reactions. As a consequence of their metabolism, strong shifts in pH and/or alkalinity are often observed, which may in turn foster or hamper carbonate supersaturation in pore waters, hence calcium carbonate precipitation [see comprehensive syntheses by Megenigal et al. (2003) and Burdige (2006, Chapters 7 and 16) and Soetaert et al. (2007)]. Most of the known bio-induced or bio-mediated chemical reactions leading to authigenic carbonate precipitation function under primarily anaerobic conditions. Two anaerobic, microbially-mediated reactions studied best in the shallow subsurface are bacterial sulfate-reduction (Berner, 1980; Jørgensen, 1982; Burdige, 2006) and sulfate-dependent anaerobic oxidation of methane (AOM), conjointly operated by consortia of anaerobic methanoxidizing archaea and sulfate-reducing bacteria (e.g., Hinrichs et al., 1999; Boetius et al., 2000). Basically, the reactions of sulfate reduction and anaerobic oxidation of methane can be summarized by the following equations:



In such equations, CH_2O is a simplified, conventional way to represent organic matter. The alkalinity generated by both reactions may favor precipitation of authigenic carbonates in the shallow subsurface of the seafloor (Berner, 1980):



The $\delta^{34}\text{S}$ values for the pyrites extracted from the patch reefs range between $-42.9\text{\textperthousand}$ and $-35.1\text{\textperthousand}$. The $\delta^{34}\text{S}$ value for the Late Jurassic seawater is in average $+15\text{\textperthousand}$ (Prokoph et al., 2008). The significant sulfur isotope fractionation between the Jurassic seawater values and pyrite strongly suggests that bacterial sulfate reduction operated within a comparatively infinite sulfate reservoir, that is, most likely at or very close to the sediment–water interface. Among anaerobic processes, sulfate reduction is most commonly involved into diagenetic carbonate precipitation because sulfate ions are abundant in seawater and sediment pore water (e.g., Jørgensen, 1982; Scotchman, 1991; Peckmann and Thiel, 2004; Pierre et al., 2012).

Based on the abundant literature devoted to microbial activity and authigenic carbonates formed at seep sites (e.g., Hinrichs et al., 1999; De Craen et al., 1999; Boetius et al., 2000; Peckmann and Thiel, 2004; Gontharet et al., 2007, 2009; Ge et al., 2010; Birgel et al., 2011; Chevalier et al., 2011, to mention just a few recent papers), we interpret the localized isotopic anomalies corresponding

to the patch reefs as scattered spots where bacterial activity was fueled by seepage of hydrocarbon-rich fluids, but no (biomarker) evidence for AOM was found (see above). In the patch reefs, specific sulfate-reducing bacteria may have processed the seeping hydrocarbons, as some of them are known to degrade *n*-alkanes and *n*-alkenes (see Grossi et al., 2008 and references therein). Further, activity of sulfate-reducing bacteria is evidenced by abundant pyrite framboids and their specific isotopically-depleted sulfur isotopes. Similar observations were made in other authigenic precipitates, namely phosphorites, where also additional biomarker evidence for sulfate reducers was found (Arning et al., 2009). As a consequence of bacterial activity of sulfate reducers, a localized alkalinity increase led to carbonate precipitation. The $\delta^{13}\text{C}$ signature of the authigenic carbonate was in contrast to the values found for the enclosing marls and that of the shells of the bivalves. These bivalves may have been feeding on the bacterial biomass, but since oysters are so far not known to feed on bacteria or live in chemosymbiosis, they may have simply used the authigenic carbonate as a firm ground. The fact that the $\delta^{13}\text{C}$ is not significantly depleted suggests that the carbonates of the matrix resulted from a mixture of two sources: 1) a light C source such as organic matter remineralization (or even hydrocarbon oxidation) and, 2) a seawater DIC source. The fact that the sparry shell fillings yield more negative $\delta^{18}\text{O}$ values than those of the microsparitic matrix or shells suggests a carbonate precipitation during later diagenesis, with pore-space fluids that had evolved from seawater.

6.2. Patch reefs vs. Beauvoisin pseudo-bioherms

It is tempting to compare the patch reefs of the Boulonnais to the Late-Jurassic pseudo-bioherms of the Beauvoisin site (Vocontian Trough, South-Eastern France), investigated by Bourreau (1977), Gaillard et al. (1985), Gaillard and Rolin (1986), Rolin et al. (1990), Peckmann et al. (1999), Gay (2002), Louis-Schmid et al. (2007) and Tribovillard et al. (2013). These pseudo-bioherms (fossiliferous calcareous bodies with a bioherm shape but no reef-building organisms forming a significant relief at the sediment–water interface) are included in the Terres Noires Formation, a 2500 m-thick marlstone accumulation dated of Bathonian–Kimmeridgian age, and deposited under hemi-pelagic conditions (Tribovillard and Dureux, 1986; Tribovillard, 1988). The pseudo-bioherms are located approximately along or very close to synsedimentary faults that were active during the deposition of the Terres Noires (Gaillard and Rolin, 1988). The proximity of the carbonate precipitates to fault systems is a similarity found as well in the patch reefs. The pseudo-bioherms are lens- or column-shaped carbonate bodies interbedded within marlstones. Their size is (pluri-) metric for both diameter and height. Biogenic remains include mainly numerous bivalve shells (lucinids), pellets and planktonic foraminifera (protoglobigerinids). Gaillard et al. (1992), Peckmann et al. (1999), Louis-Schmid et al. (2007) and Tribovillard et al. (2013) reported isotope data obtained from pseudo-bioherms, carbonate nodules and lucinid shells of Beauvoisin. The limestones are depleted in ^{13}C with $\delta^{13}\text{C}$ ranging from $-24.6\text{\textperthousand}$ to $-9.7\text{\textperthousand}$ PDB. In addition, the typical molecular signature of the AOM consortia was identified (Peckmann et al., 1999). Comparing the sedimentological, faunal and geochemical features of the pseudo-bioherms of Beauvoisin to those of ancient or present sites of hydrocarbon seepage, Rolin et al. (1990) and Gaillard et al. (1992) interpreted the pseudo-bioherms as formed at ancient cold seeps, with carbonate masses and nodules authigenically resulting from bacterial activity, fueled by fluids circulating along synsedimentary faults.

To what extent can the patch reefs be compared to the pseudo-bioherms? Both the Jurassic patch reefs and Beauvoisin pseudo-

bioherms are rich in bivalves, though different groups of bivalves are preserved in the carbonates. In Beauvoisin, lucinids are the only bivalves identified, these bivalves are known to live with endosymbiotic bacteria (Rolin et al., 1990; Gaillard et al., 1992; Callender and Powell, 2000), allowing them to endure anoxic conditions, which is not the case with the patch reef oysters. In addition, the $\delta^{13}\text{C}$ values of the pseudo-bioherms are much more depleted than the ones in the patch reefs. Furthermore, molecular signatures of the AOM-performing consortia were identified in the pseudo-bioherms and were not found in patch reefs (Peckmann et al., 1999). Consequently, AOM cannot be put forward as carbonate forming process in the patch reefs and is in great contrast to the pseudo-bioherms of Beauvoisin. Consequently, activity of sulfate reducing bacteria solely, without AOM involvement, must be retained for the patch reefs. Nevertheless, the major similarity of both the patch reefs and the pseudo-bioherms is their occurrence in the vicinity of synsedimentary faults. During the Late Jurassic, the Boulonnais area was affected by synsedimentary faulting in relation with the rifting of the Atlantic Ocean. The patch reefs are concentrated at stratigraphic levels that were affected by synsedimentary tectonics as well. More conspicuously, patch reefs are observed on a synsedimentary fault plane and on the surface of beds softly deformed by synsedimentary extensional movements (Figs. 5 and 6). Lastly, fluid expulsions associated to synsedimentary tectonics were also held responsible for rendering depositional conditions prone to sulfate reduction, inducing the rapid, authigenic formation of the carbonate beds of the overlying Bancs Jumeaux Formation (Fig. 1C; Tribouillard et al., 2012). Thus, synsedimentary fluid expulsion causing authigenic carbonate precipitation by activity of hydrocarbon-degrading sulfate reducing bacteria is a recurrent feature of the Boulonnais during the latest Jurassic.

7. Conclusion

The late-Jurassic formations of the Boulonnais area show carbonates, either patch reefs or carbonate beds, yielding common facies and microfacial features. Their common and widespread occurrence could be misinterpreted without stable isotope data, pointing to their authigenic origin. The formation of the authigenic carbonate phases was induced by an increase of alkalinity, closely associated to the activity of hydrocarbon-degrading, sulfate reducing bacteria. The presence and activity of sulfate reducing bacteria in early diagenesis was most probably induced and fueled by seepage of hydrocarbon-rich fluids, ascending along synsedimentary fault planes from deeper, organic-rich layers that structured the Boulonnais.

Acknowledgment

We thank Florent Barbicot for his constant support with isotope analyses, Pauline Manet, formerly master student and the members of the technical staff of the Géosystèmes Lab, namely, Marion Delattre, Monique Gentric, Sylvie Regnier, Sandra Ventalon, Romain Abraham and Philippe Recourt. We thank Rudy Swennen and Olivier Lacombe, guest editors of the special Issue of Marine and Petroleum Geology. We are indebted to our reviewers — Martin Blumenberg and an anonymous referee — as well as Rudy Swennen for their scientific expertise and editorial work that helped us improve significantly the paper.

References

- Al-Ramadan, K., Morad, S., Proust, J.-N., Al-Aasm, I., 2005. Distribution of diagenetic alterations in siliciclastic shoreface deposits within a sequence stratigraphic framework: evidence from the upper Jurassic Boulonnais, NW France. *J. Sediment. Res.* 75, 943–959.
- Aloisi, G., Bouloubassi, I., Heijls, S.K., Pancost, R.D., Pierre, C., Sanninghe Damste, J.S., Gottschal, J.C., Forney, L.J., Rouchy, J.-M., 2002. CH₄-consuming microorganisms and the formation of carbonate crusts at cold seeps. *Earth Planet. Sci. Lett.* 203, 195–203.
- Arning, E.T., Birgel, D., Brunner, B., Peckmann, J., 2009. Bacterial formation of phosphatic laminites off Peru. *Geobiology* 7, 295–307.
- Bates, R.L., Jackson, J.A., 1987. *Glossary of Geology*, third ed. American Geological Institute, p. 788.
- Beeley, H.S., Norton, M.G., 1998. The structural development of the Central English Channel High — constraints from section restoration. In: Underhill, J.R. (Ed.), *Development, Evolution and Petroleum Geology of the Wessex Basin*, Geological Society, London, Special Publications, vol. 133, pp. 283–298.
- Berner, R.A., 1980. *Early Diagenesis — a Theoretical Approach*. Princeton University Press, p. 241.
- Birgel, D., Feng, D., Roberts, H.H., Peckmann, J., 2011. Changing redox conditions at cold seeps as revealed by authigenic carbonates from Alaminos Canyon, northern Gulf of Mexico. *Chem. Geol.* 285, 82–96.
- Birgel, D., Thiel, V., Hinrichs, K.-U., Elvert, M., Campbell, K.A., Reitner, J., Farmer, J.D., Peckmann, J., 2006. Lipid biomarker patterns of methane-seep microbialites from the Mesozoic convergent margin of California. *Org. Geochem.* 37, 1289–1302.
- Birgel, D., Elvert, M., Han, X., Peckmann, J., 2008. ^{13}C -depleted biphytanic diacids as tracers of past anaerobic oxidation of methane. *Org. Geochem.* 39, 152–156.
- Boetius, A., Ravenschlag, K., Schubert, C.J., Rickert, D., Widdel, F., Gieseke, A., Amann, R., Jørgensen, B.B., Witte, U., Pfannkuche, O., 2000. A marine microbial consortium apparently mediating anaerobic oxidation of methane. *Nature* 407, 623–626.
- Bourseau, J.P., 1977. L'Oxfordien moyen à nodules des "Terres Noires" de Beauvoisin (Drôme). *Nouvelles Arch. Mus. Hist. Nat. Lyon* 15, 116.
- Bout-Roumazeilles, V., Cortijo, E., Labeyrie, L., Debrabant, P., 1999. Clay-mineral evidence of nepheloid layer contribution to the Heinrich layers in the Northwest Atlantic. *Palaogeogr. Palaeoclimatol. Palaeoecol.* 146, 211–228.
- Burdige, D.J., 2006. *Geochemistry of Marine Sediments*. Princeton University Press, p. 609.
- Butler, M., Pullan, C.P., 1990. Tertiary structures and hydrocarbon entrapment in the Weald Basin of southern England. In: Hardman, R.F.P., Brooks, J. (Eds.), *Tectonic Events Responsible for Britain's Oil and Gas Reserves*, Geological Society, London, Special Publications, vol. 55, pp. 371–391.
- Callender, R., Powell, E.N., 2000. Long-term history of chemoautotrophic clam-dominated faunas of petroleum seeps in the Northwestern Gulf of Mexico. *Facies* 43, 177–204.
- Chevalier, N., Bouloubassi, I., Birgel, D., Crémère, A., Taphanel, M.-H., Pierre, C., 2011. Authigenic carbonates at cold seeps in the Marmara Sea (Turkey): a lipid biomarker and stable carbon and oxygen isotope investigation. *Mar. Geol.* 288, 112–121.
- De Craen, M., Swennen, R., Keppens, E.M., Macaulay, C.I., Kiriaikoulakis, K., 1999. Bacterially mediated formation of carbonate concretions in the Oligocene Boom Clay of Northern Belgium. *J. Sediment. Res.* 69, 1098–1106.
- Deconinck, J.-F., Geyssant, J.R., Proust, J.-N., Vidier, J.P., 1996. Sédimentologie et biostratigraphie des dépôts kimméridgiens et tithoniens du Boulonnais. *Ann. Soc. Géol. Nord* 4, 157–170.
- Delecat, S., Peckmann, J., Reitner, J., 2001. Non-rigid cryptic sponges in oyster patch reefs (Lower Kimmeridgian, Langenberg/Oker, Germany). *Facies* 45, 231–254.
- Folk, R.L., Chafetz, H.S., 2000. Bacterially induced microscale and nanoscale carbonate precipitates. In: Riding, R.E., Awramik, S.M. (Eds.), *Microbial Sediments*. Springer, pp. 40–49.
- Fürsch, F.T., 1981. Salinity-controlled benthic associations from the Upper Jurassic of Portugal. *Lethaia* 14, 203–223.
- Gaillard, C., Bourseau, J.P., Boudeulle, M., Pailleret, P., Rio, M., Roux, M., 1985. Les pseudobiohermes de Beauvoisin (Drôme): un site hydrothermal sur la marge téthysienne l'Oxfordien? *Bull. Soc. Géol. France* 8 (1), 69–78.
- Gaillard, C., Rio, M., Rolin, Y., 1992. Fossil chemosynthetic communities related to vents or seeps in sedimentary basins: the pseudobioherms of south-eastern France compared to other world examples. *Palaeos* 7, 451–465.
- Gaillard, C., Rolin, Y., 1986. Paléobiocoénoses susceptibles d'être liées à des sources sous-marines en milieu sédimentaire. L'exemple des Terres Noires (SE France) et des tectepe buttes de la Pierre Shale Formation (Colorado, U.S.A.). *C. R. Acad. Sci. Paris* 303, 1503–1508.
- Gaillard, C., Rolin, Y., 1988. Relation entre tectonique synsédimentaire et pseudobiohermes (Oxfordien de Beauvoisin-Drôme-France). Un argument supplémentaire pour interpréter les pseudobiohermes comme formés au droit de sources sous-marines. *C. R. Acad. Sci. Paris* 307, 1265–1270.
- Gay, A., 2002. Les marqueurs géologiques de la migration et de l'expulsion des fluides sédimentaires sur le plancher des marges passives matures. Exemples dans le Bassin du Congo, vol. 1, p. 426 (Thèse Université de Lille).
- Ge, L., Jiang, S.-Y., Swennen, R., Yang, T., Yang, J.-H., Wu, N.-Y., Liu, J., Chen, D.H., 2010. Chemical environment of cold seep carbonate formation on the northern continental slope of South China Sea: evidence from trace and rare earth element geochemistry. *Mar. Geol.* 277, 21–30.
- Geyssant, J.R., Vidier, J.-P., Herbin, J.-P., Proust, J.N., Deconinck, J.-F., 1993. Biostratigraphie et paléoenvironnement des couches de passage Kimméridgien/Tithonien du Boulonnais (Pas de Calais): nouvelles données paléontologiques (ammonites), organisation séquentielle et contenu en matière organique. *Géol. France* 4, 11–24.

- Gontharet, S., Pierre, C., Blanc-Valleron, M.-M., Rouchy, J.M., Fouquet, Y., Bayon, G., Foucher, J.P., Woodside, J., Mascle, J., The Nautinil Scientific Party, 2007. Nature and origin of diagenetic carbonate crusts and concretions from mud volcanoes and pockmarks of the Nile deep-sea fan (eastern Mediterranean Sea). Deep Sea Res. Part II: Top. Stud. Oceanogr. 54, 1292–1311.
- Gontharet, S., Stadnitskaia, A., Bouloubassi, I., Pierre, C., Sinninghe Damsté, J.S., 2009. Palaeo methane-seepage history traced by biomarker patterns in a carbonate crust, Nile deep-sea fan (eastern Mediterranean Sea). Mar. Geol. 261, 105–113.
- Grossi, V., Cravo-Laureau, C., Guyoneaud, R., Ranchou-Peyrusse, A., Hirschler-Réa, A., 2008. Metabolism of *n*-alkanes and *n*-alkenes by anaerobic bacteria: a summary. Org. Geochem. 39, 1197–1203.
- Hansen, D.L., Blundell, D.J., Nielsen, S.B., 2002. A model for the evolution of the Weal Basin. Bull. Geol. Soc. Denmark 49, 109–118.
- Heim, C., Schulke, I., 1998. A coral-microbialite patch reef from the Late Jurassic (Florigemma-Bank, Oxfordian) of NW Germany (Süntel Mountains). Facies 39, 75–104.
- Hinrichs, K.-U., Hayes, J., Sylva, S., Brewer, P., DeLong, E., 1999. Methane-consuming archaeabacteria in marine sediments. Nature 398, 802–805.
- Jørgensen, B.B., 1982. Mineralization of organic matter in the sea bed — the role of sulphate reduction. Nature 296, 643–645.
- Louis-Schmid, B., Rais, P., Logvinovich, D., Bernasconi, S.M., Weissert, H., 2007. Impact of methane seeps on the local carbon-isotope record: a case study from a Late Jurassic hemipelagic section. Terra Nova 19, 259–265.
- Mansy, J.-L., Guennoc, P., Robaszynski, F., Amedro, F., Auffret, J.-P., Vidier, J.-P., Lamarche, J., Lefèvre, D., Sommè, J., Brice, D., Mistiaen, B., Prud'homme, A., Rohart, J.-C., Vachard, D., 2007. Notice explicative, carte géologique de la France (1/50 000), feuille Marquise, second ed. BRGM, Orléans, p. 213.
- Mansy, J.-L., Manby, G.M., Averbuch, O., Everaerts, M., Bergerat, F., Van Vliet-Lanoë, B., Lamarche, J., Vandycke, S., 2003. Dynamics and inversion of the Mesozoic Basin of the Weald-Boulonnais area: role of basement reactivation. Tectonophysics 373, 161–179.
- McCrea, J.M., 1950. On the isotopic chemistry of carbonates and a paleotemperature scale. J. Chem. Phys. 18, 849–857.
- Megonigal, J.P., Hines, M.E., Visscher, P.T., 2003. Anaerobic metabolism: linkages to trace gases and aerobic processes. In: Schlessinger, W.H. (Ed.), Biogeochemistry. In: Holland, H.D., Turekian, K.K. (Eds.), Treatise on Geochemistry, vol. 8. Elsevier-Pergamon, Oxford, pp. 317–424.
- Minguely, B., Averbuch, O., Patin, M., Rolin, D., Hanot, F., Bergerat, F., 2010. Inversion tectonics at the northern margin of the Paris basin (Northern France): new evidence from seismic profiles and boreholes interpolation in the Artois area. Bull. Soc. Géol. France 181 (5), 429–442.
- Newell, A.J., 2000. Fault activity and sedimentation in a marine rift basin (Upper Jurassic, Wessex Basin, UK). J. Geol. Soc. 157, 83–92.
- Peckmann, J., Thiel, V., 2004. Carbon cycling at ancient methane-seeps. Chem. Geol. 205, 443–467.
- Peckmann, J., Thiel, V., Michaelis, W., Clari, P., Gaillard, C., Martire, L., Reitner, J., 1999. Cold seep deposits of Beauvoisin (Oxfordian; southeastern France) and Marmorito (Miocene; northern Italy): microbially authigenic carbonates. Int. J. Earth Sci. 88, 60–75.
- Pierre, C., Blanc-Valleron, M.-M., Demange, J., Boudouma, O., Foucher, J.-P., Pape, T., Himmler, T., Fekete, N., Spiess, V., 2012. Authigenic carbonates from active methane seeps offshore southwest Africa. Geo-Mar. Lett. 32, 501–513.
- Prokoph, A., Shields, G.A., Veizer, J., 2008. Compilation and time-series analysis of a marine carbonate $\delta^{18}\text{O}$, $\delta^{13}\text{C}$, $^{87}\text{Sr}/^{86}\text{Sr}$ and $\delta^{34}\text{S}$ database through Earth history. Earth-Sci. Rev. 87, 113–133.
- Proust, J.-N., Deconinck, J.-F., Geyssant, J.R., Herbin, J.-P., Vidier, J.-P., 1995. Sequence analytical approach to the Upper Kimmeridgian–Lower Tithonian storm-dominated ramp deposits of the Boulonnais (Northern France) – a landward time-equivalent to offshore marine source rocks. Geol. Rundsch. 84, 255–271.
- Ramanampisoa, L., Bertrand, P., Disnar, J.R., Lallier-Vergès, E., Pradier, B., Tribouillard, N., 1992. High-resolution study of an organic-carbon cycle in the Kimmeridge Clays of Yorkshire (Great Britain) – preliminary results of organic geochemistry and petrography. C. R. Acad. Sci. 314 (II), 1493–1498.
- Rolin, Y., Gaillard, C., Roux, M., 1990. Ecologie des pseudobiohermes des Terres Noires jurassiques liés à paléo-sources sous-marines. Le site oxfordien de Beauvoisin (Drôme, Bassin du Sud-Est, France). Palaeogeogr. Palaeoclimatol. Palaeocol. 80, 79–105.
- Scotchman, I.C., 1991. The geochemistry of concretions from the Kimmeridge clay formation of southern and eastern England. Sedimentology 38, 79–106.
- Soetaert, K., Hofmann, A.F., Middelburg, J.J., Meysman, F.J.R., Greenwood, J., 2007. The effect of biogeochemical processes on pH. Mar. Chem. 105, 30–51.
- Taylor, S.P., Sellwood, B.W., 2002. The context of lowstand events in the Kimmeridgian (Late Jurassic) sequence stratigraphic evolution of the Wessex–Weald Basin, Southern England. Sediment. Geol. 151, 89–106.
- Tribouillard, N., Ramdani, A., Trentesaux, A., 2005. Controls on organic accumulation in Late Jurassic shales of Northwestern Europe as inferred from trace-metal geochemistry. In: Harris, N. (Ed.), The Deposition of Organic-Carbon-Rich Sediments: Models, Mechanisms, and Consequences, SEPM Special Publication, vol. 82, pp. 145–164.
- Tribouillard, N.-P., 1988. Géochimie organique et minérale dans les Terres Noires calloviennes et oxfordiennes du bassin dauphinois (France SE): mise en évidence de cycles climatiques. Bull. Soc. Géol. France 8 (5), 141–150.
- Tribouillard, N.-P., Ducreux, J.-L., 1986. Mise en évidence de cycles de 100 000 et 400 000 ans dans les Terres Noires du Callovien–Oxfordien de la région de Buis-les-Baronnies (France S-E). C. R. Acad. Sci. Paris II (20), 1508–1512 t. 303.
- Tribouillard, N., Armynot du Châtelet, E., Gay, A., Barbicot, F., Sansjofre, P., Potdevin, J.-L., 2013. Geochemistry of cold seepage-impacted sediments: Per-ascensum or per-descensum trace metal enrichment? Chem. Geol. 340, 1–12.
- Tribouillard, N., Bialkowski, A., Tyson, R.V., Vergès, E., Deconinck, J.-F., 2001. Organic facies and sea level variation in the Late Kimmeridgian of the Boulonnais area (northernmost France). Mar. Petrol. Geol. 18, 371–389.
- Tribouillard, N., Sansjofre, P., Ader, M., Trentesaux, A., Averbuch, O., Barbicot, F., 2012. Early diagenetic carbonate bed formation at the sediment–water interface triggered by synsedimentary faults. Chem. Geol. 300/301, 1–13.
- Tribouillard, N., Trentesaux, A., Ramdani, A., Baudin, F., Riboullau, A., 2004. Contrôles de l'accumulation de matière organique dans la Kimmeridge clay formation (Jurassique supérieur, Yorkshire, G.B.) et son équivalent latéral du Boulonnais: l'apport des éléments traces métalliques. Bull. Soc. Géol. France 175, 491–506.
- Underhill, J.R., Paterson, S., 1998. Genesis of Tectonic inversion structures: seismic evidence for the development of key structures along the Purbeck-Isle of Wight Monocline. J. Geol. Soc. 155, 975–992.
- Veizer, J., Ala, D., Azmy, K., Bruckschen, P., Buhl, D., Bruhn, F., Carden, G.A.F., Diener, A., Ebnet, S., Godderis, Y., Jasper, T., Korte, C., Pawellek, F., Podlaha, O.G., Strauss, H., 1999. $^{87}\text{Sr}/^{86}\text{Sr}$, ^{13}C and ^{18}O evolution of Phanerozoic seawater. Chem. Geol. 161, 59–88.
- Wignall, P.B., 1991. Test of the concepts of sequence stratigraphy in the Kimmeridgian (Late Jurassic) of England and northern France. Mar. Petrol. Geol. 8, 430–441.
- Wignall, P.B., Newton, R., 2001. Black shales on the basin margin: a model based on examples from the Upper Jurassic of the Boulonnais, northern France. Sediment. Geol. 144, 335–356.
- Williams, C.J., Hesselbo, S.P., Jenkyns, H.C., Morgans-Bell, H.S., 2001. Quartz silt in mudrocks as a key to sequence stratigraphy (Kimmeridge Clay Formation, Late Jurassic, Wessex Basin, UK). Terra Nova 13, 449–455.
- Wilmsen, M., Fürsch, F.T., Seyed-Emami, K., Majidifar, M., Zamani-Pedram, M., 2010. Facies analysis of a large-scale Jurassic shelf-lagoon: the Kamar-e-Mehdi Formation of east-central Iran. Facies 56, 59–87.